

(NASA-CR-199138) THE
RECONSTRUCTION OF IMAGES DISTORTED
BY HYPERSONIC TURBULENCE (Alabama
Univ.) 4 p

N95-71645

Unclass

Z9/19 0063090

THE RECONSTRUCTION OF IMAGES DISTORTED BY HYPERSONIC TURBULENCE

by

Constantine Katsinis

Electrical and Computer Engineering Department

University of Alabama in Huntsville

Huntsville, AL 35899

70-1-12
63590

ABSTRACT

The performance of sensors aboard platforms that travel at hypersonic speeds within the atmosphere is degraded by image distortion partially due to turbulent mixing of coolant gases in front of the sensor window. To study this degradation, a sequence of experiments was performed that produced a number of distorted images using different mixtures of turbulent gases. This paper describes these experiments and presents image processing algorithms, based on shifted-average techniques that are used to reconstruct the original image. The quality of the reconstruction depends on the particular gas combination and on the number of images used by the reconstruction algorithm.

INTRODUCTION

Hypervelocity vehicles use infrared sensors to detect, recognize and track targets. The environment of hypersonic flight is such that sensors must be protected from high temperatures by windows. There is no window material available yet that can survive for long in this environment and therefore the window itself must be protected and cooled by a very low temperature coolant gas which is ejected over the window. This mechanism cools the window sufficiently but, as the coolant gas and the atmosphere come together, a turbulent mixing layer is formed which creates optical distortions that severely affect the image quality. The properties of the turbulence are under investigation in an effort to accurately interpret images collected through cooled windows. A second source of image distortion is due to the gradient of the index of refraction in front of the window. The high velocity flow over the vehicle creates a low-density, high-temperature region behind the bow shock and the coolant gas directly over the window creates a higher-density, low-temperature region. The density difference in these two regions results in the index of refraction gradient.

To approximate these phenomena and create a mixing layer that matches the real flight conditions, an experimental laboratory setup was created [1,2,3]. This setup contained a chamber formed by two parallel windows in which a high pressure coolant gas and a low pressure backfill gas were mixed through a nozzle. By adjusting the pressure of the backfill gas and the static pressure in the test area, the density difference in the mixing stream was controlled. The setup also included the necessary optics to produce a collimated laser beam of light, that approximated an incoming target. The beam was directed into the mixing area, 2 inches away

from the nozzle and was detected on the other side by a high speed video camera which captured 320 images at a rate of 370 images per second. Each image was created by a 300 nsec laser light pulse. The image of the light source without any turbulence is shown in Figure 1. Figure 2 shows three consecutive images distorted by turbulence.

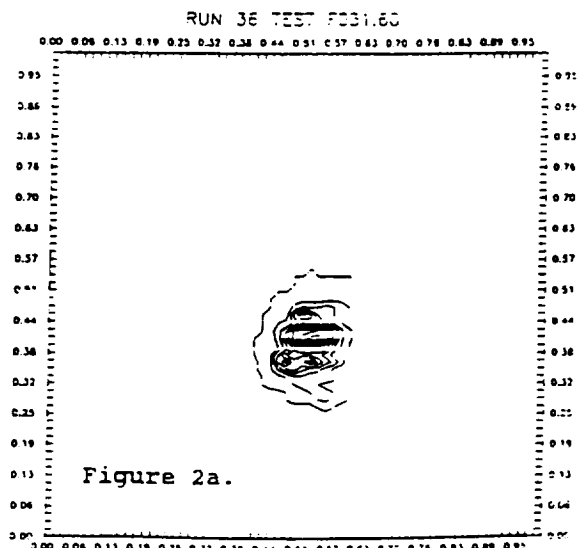
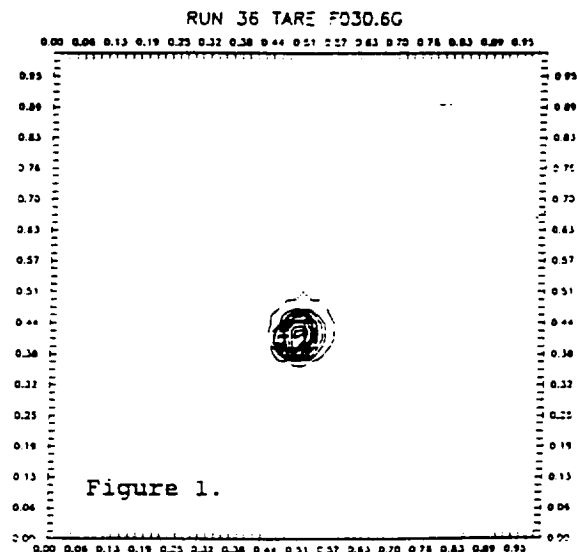
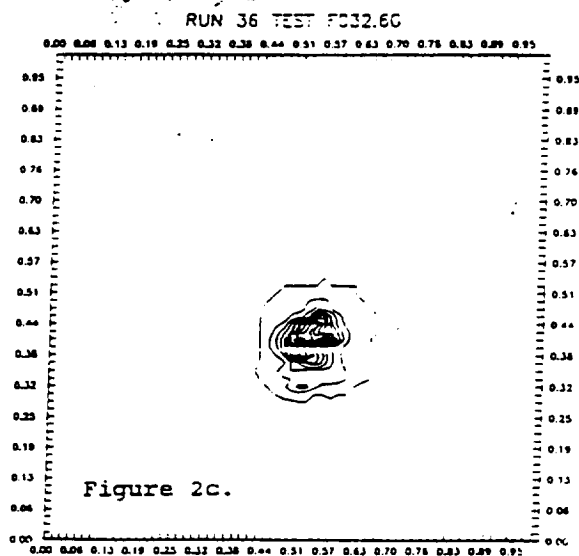
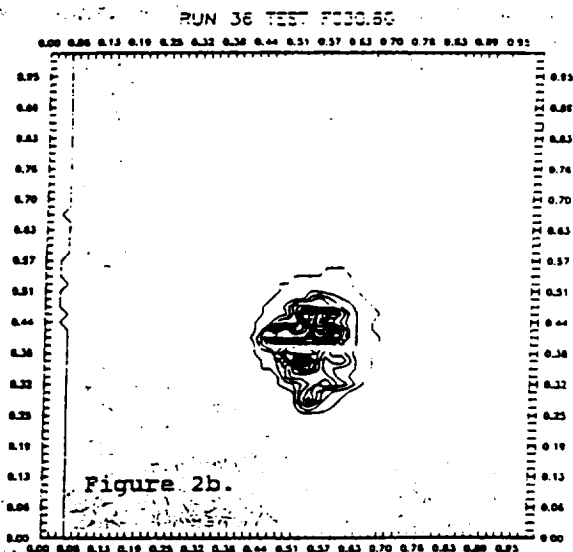


IMAGE PROCESSING

The individual images $g_i(x,y)$ recorded by the camera can be expressed as a convolution of the original undistorted image $f(x,y)$ with a point spread function $h_i(x,y)$ that characterizes the mixing area



$$g_i(x,y) = f(x,y) \otimes h_i(x,y) + c_i(x,y) \quad (1)$$

$$i = 1, \dots, N$$

where $c_i(x,y)$ represents any additive contamination and N is the total number of images. The regular average of a sequence of images is

$$g_d(x,y) = \langle g_i(x,y) \rangle \quad (2)$$

If each image in the sequence is shifted before averaging such that its brightest pixel appears at a specific image coordinate, then a shifted - average is obtained

$$g_s(x,y) = \langle g_i(x+dx_i, y+dy_i) \rangle \quad (3)$$

Combining Eq. (1) and (3) we have

$$g_s = \langle f(x,y) \otimes h_i(x+dx_i, y+dy_i) + c_i(x+dx_i, y+dy_i) \rangle$$

$$= f(x,y) \otimes h_s(x,y) + c_s(x,y) \quad (4)$$

where $h_s(x,y) = \langle h_i(x+dx_i, y+dy_i) \rangle$ and $c_s(x,y)$ is the shifted - average of the additive contamination.

If $c_s(x,y)$ is small, then Eq. (4) represents a convolution of the original image with an unknown point spread function.

An estimate of $h_s(x,y)$ can be obtained by observing a point source which can be a target at a large distance

$$h_s(x,y) = t_s(x,y) \quad (5)$$

where $t_s(x,y)$ is obtained from Eq. (4) with $f(x,y)$ replaced by $\delta(x,y)$. An estimate of $f(x,y)$ is the result of Wiener filtering of $g_s(x,y)$

$$g_e(x,y) = F^{-1}[G_s(u,v)/(T_s(u,v)+\epsilon)] \quad (6)$$

where $G_s(u,v)$ and $T_s(u,v)$ are the Fourier transforms of $g_s(x,y)$ and $t_s(x,y)$ respectively. The Wiener filter provides an estimate of $f(x,y)$ that attempts to remove the distortion due to the turbulent medium. To isolate this effect, Eq. (4) can be rewritten as

$$g_s(x,y) = f(x,y) \otimes h_s(x,y) \otimes h_o(x,y) + c_s(x,y) \quad (7)$$

where $h_s(x,y)$ represents the effect of the medium and $h_o(x,y)$ represents the effect of the object on the distorted image. As the object tends to become a single point, $h_o(x,y)$ approaches $\delta(x,y)$. The Wiener filter removes the effect of $h_s(x,y)$ and therefore

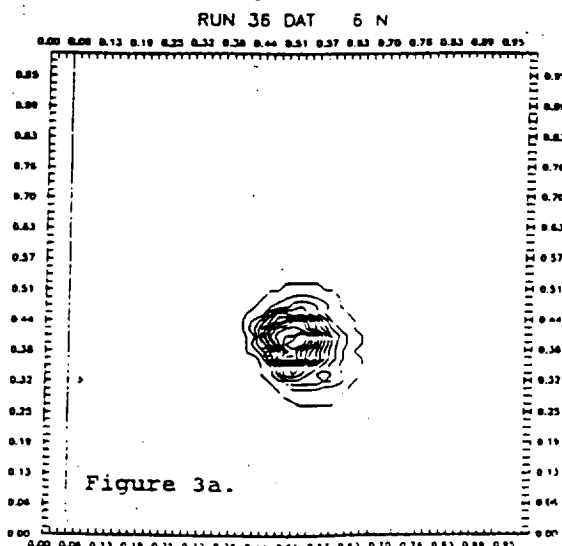
$$g_e(x,y) = f(x,y) \otimes h_o(x,y) + c_s(x,y) \quad (8)$$

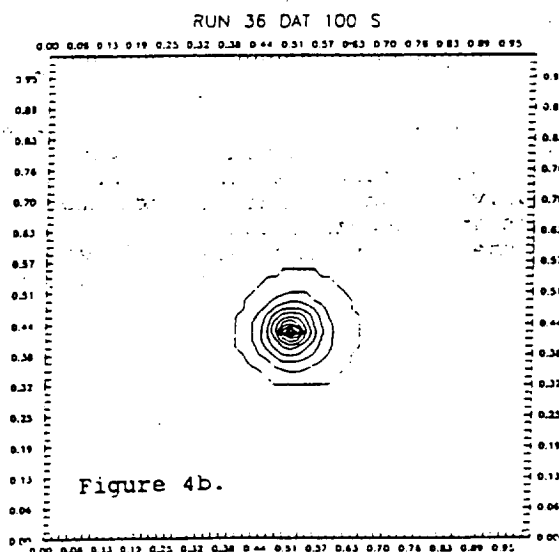
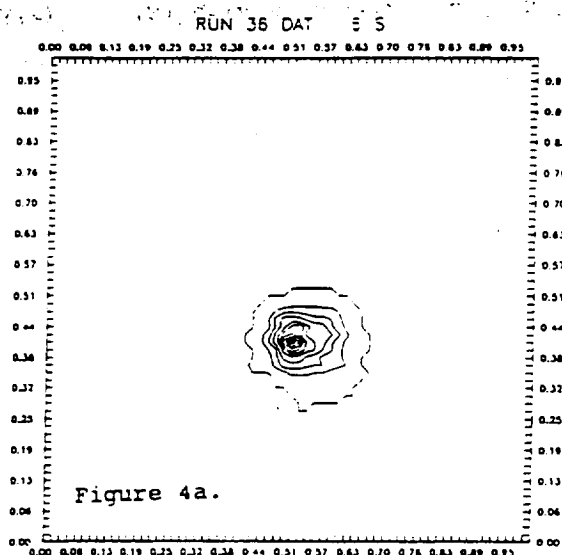
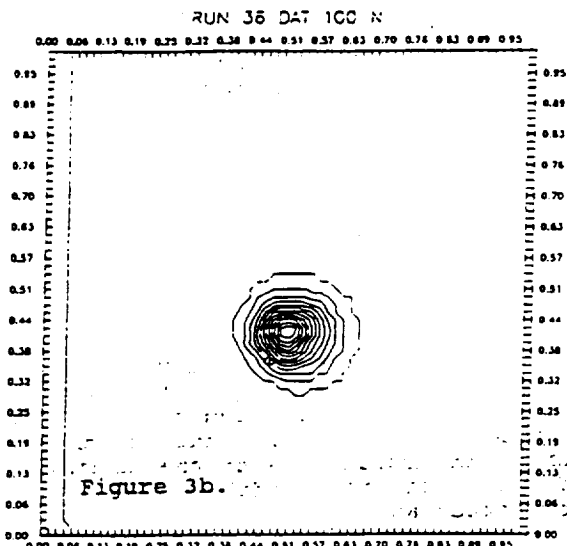
is the expression of the estimate of the original image.

EXPERIMENTAL RESULTS

The processing described above was applied on a sequence of images that approximate the distortion of a target image due to the mixing of helium coolant and argon backfill gases as a vehicle travels at approximately 2 Mach. The image of the target with no distortion is shown in Figure 1. Three successive distorted images are shown in Figure 2.

If a number of successive images are simply averaged, the result is a diffuse area in the image with very little information. Figure 3 shows the result of simply averaging 6 or 100 successive images. Shifting each successive image so that its brightest pixel appears at a specific location in the image, and then averaging all shifted images, results in a more precise image. Figure 4

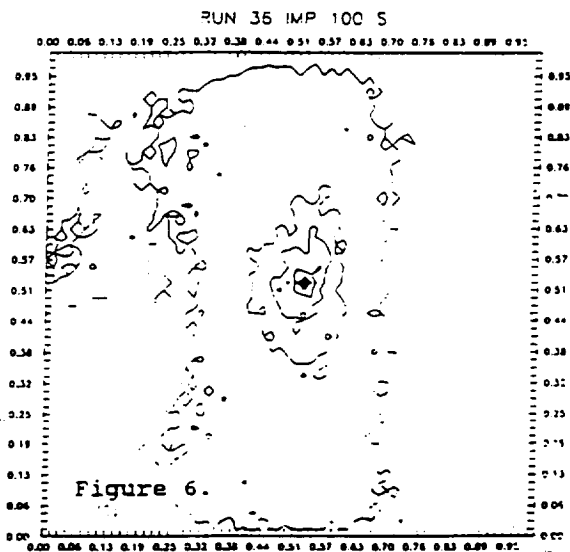
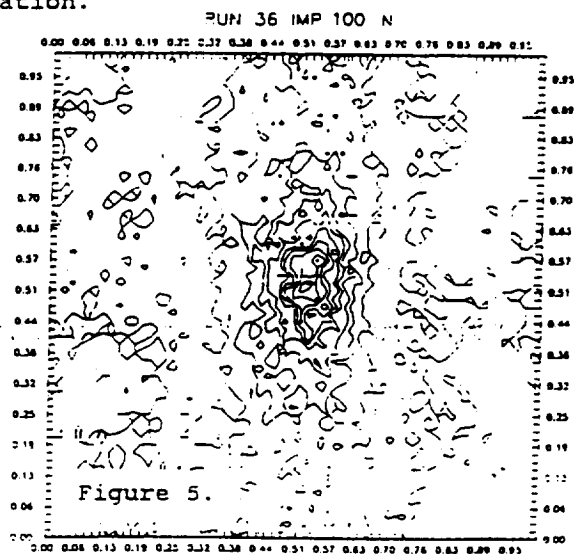




shows the results of shifted - averaging using 6 or 100 successive images.

To estimate the point spread function of the mixing layer, a point source would have to be used. In these experiments though, since both the original image $f(x,y)$ and the distorted images $g_i(x,y)$ are known, the point spread function is estimated from them. To minimize any correlation effects, the point spread function is estimated using the last

block of images in the 320 - image sequence, and is used in the processing of the first block of images in the same sequence. Figure 5 shows the average of 100 point spread function images. Figure 6 shows the average of the same 100 point spread function images, where each image was shifted so that its brightest pixel appeared at a specific location.



Having obtained an estimate of the point spread function of the mixing layer (with and without image shifting), Eq. (6) is used to arrive at an estimate of the target image. In Eq. (6), $G_s(u,v)$ and $T_s(u,v)$ are respectively the Fourier transforms of the shifted average of a number (N_g) of distorted images $g_s(x,y)$, and the shifted average of a number (N_t) of images containing estimates of the medium point spread function $t_s(x,y)$. In these experiments, the number of images used to generate $g_s(x,y)$ and $t_s(x,y)$ was varied between 6 and 100. A second set of experiments was also performed with regular averaging being used but with no shifting. Figure 7 shows the target estimate for two cases a) $N_g = 10$, $N_t = 6$, and b) $N_g = 100$, $N_t = 100$. Figure 8 shows similar results where averaging with no shifting was used.

The results of both experiments indicate that the quality of the target image reconstruction improves as both N_g and N_t increase up to approximately 50 images.

Beyond this value there is little improvement. In that sense, Figures 7b and 8b show examples of the best reconstruction achieved by this method. It is also clear from Figures 7 and 8 that the shifted-average method yields better results than the simple average method.

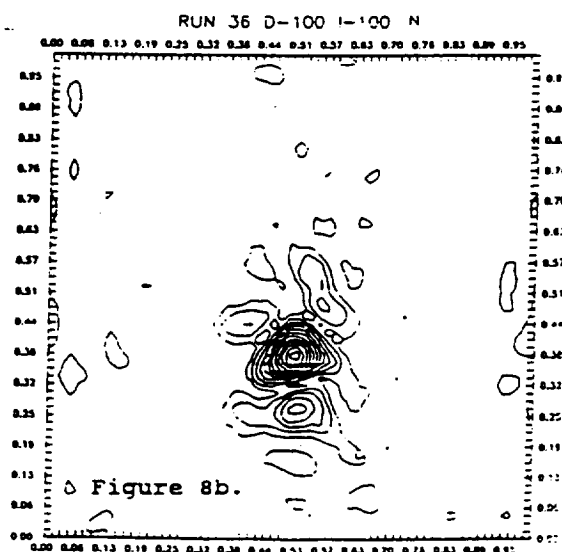
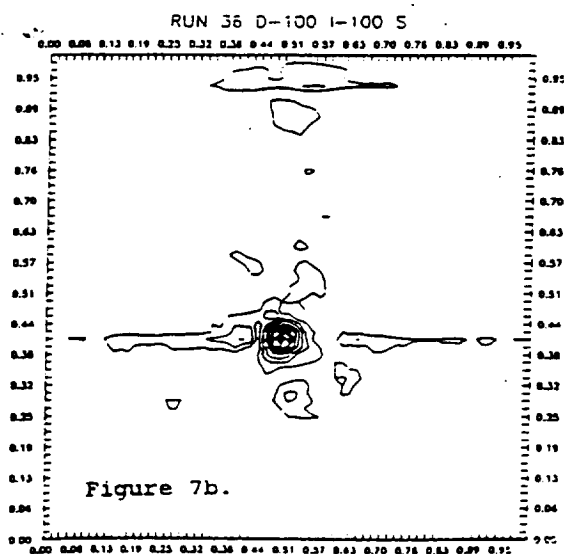
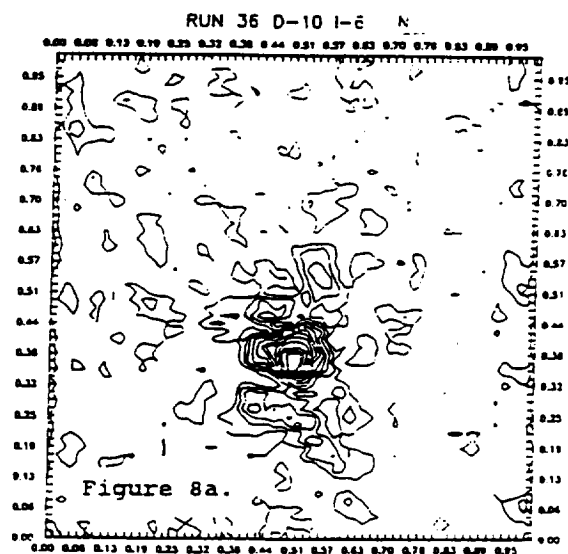
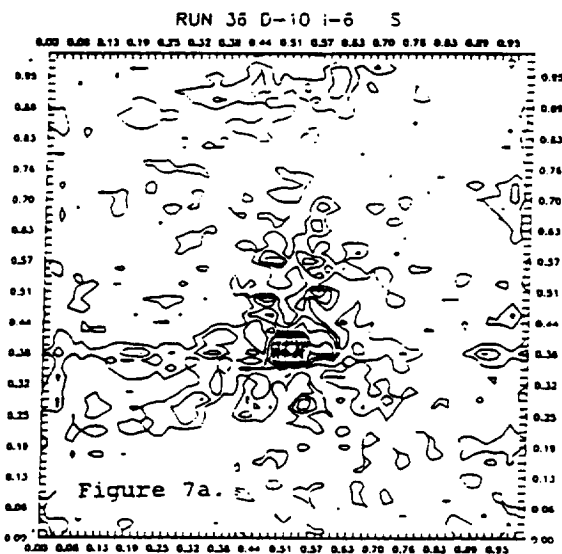
CONCLUSION

This paper describes a simple image processing technique which appears to be promising in the reconstruction of target images distorted due to propagation through a turbulent medium. Once an estimate of the point spread function of the turbulent medium is obtained by observing a target while it is still distant, a relatively small number of images can be used to obtain reconstructed estimates of the approaching target image. Compared to simple averaging, the shifted-

average method produces relatively more precise results using fewer images. The number of necessary images becomes significant when the target is moving across the field of view.

REFERENCES

1. D. Kalin, et. al., "Experimental Investigation of High Velocity Mixing / Shear Layer Aero-optic Effects", SPIE, Vol. 1326, Window and Dome Technologies and Materials II, 1990.
2. S. M. Lawson, et. al., "Aero-Optic Performance of Supersonic Mixing Layers", SPIE, Vol. 1326, Window and Dome Technologies and Materials II, 1990.
3. M. R. Banish, et. al., "Wavelength Dependence of Blur Circle Size Through Turbulent Flow", SPIE, Vol. 1326, Window and Dome Technologies and Materials II, 1990.



ACKNOWLEDGEMENT

This work was supported by U.S. Army Strategic Defense Command contract DASG60-89-C-0145.